



Pairing resonance as a normal-state spin probe in ultrathin Al films

G. Catelani

Department of Physics and Astronomy, Rutgers University, Piscataway, New Jersey 08854, USA

Y. M. Xiong, X. S. Wu,^{*} and P. W. Adams

Department of Physics and Astronomy, Louisiana State University, Baton Rouge, Louisiana 70803, USA

(Received 5 May 2009)

We present a quantitative analysis of the low-temperature, high parallel-field pairing resonance in ultrathin superconducting Al films with dimensionless conductance $g \gg 1$. In this regime we derive an analytical expression for the tunneling density-of-states spectrum from which a variety of normal-state spin parameters can be extracted. We show that by fitting tunneling data at several supercritical parallel magnetic fields we can determine all of the relevant parameters that have traditionally been obtained via fits to tunneling data in the superconducting phase. These include the spin-orbit scattering rate, the antisymmetric Landau parameter G^0 , and the orbital pair-breaking parameter.

DOI: XXXX

PACS number(s): 74.50.+r, 74.40.+k, 74.78.Db, 73.50.Fq

I. INTRODUCTION

Determining the microscopic spin parameters of paramagnetic metals has historically been a process fraught with complications and inaccuracies.^{1,2} In general, the spin response of an interacting fermionic system can be modified by spin-orbit scattering processes, electron-phonon interactions, and/or electron-electron interactions.^{3,4} These contributions to the spin susceptibility themselves can be affected by disorder,^{5,6} dimensionality,^{7,8} and the presence of interfaces.⁹ The two primary spin parameters for a paramagnetic system are the spin-orbit scattering rate and the antisymmetric $l=0$ Landau parameter G^0 . The latter accounts for the renormalization of the bare Pauli spin susceptibility due to electron-phonon and electron-electron interactions. Depending upon the sign of this parameter the effective spin moment can be larger or smaller than the bare electron value. In practice, the spin-orbit scattering rate can be obtained from the coherent backscattering contributions to the magnetoresistance of moderately disordered nonsuperconducting films or by parallel magnetic field studies of thin superconducting films. The Fermi-liquid parameter G^0 , however, is more difficult to determine accurately. In principle, it can be extracted from low-temperature measurements of the spin susceptibility χ and the heat capacity γ from which the respective corresponding density of states $N(\chi)$ and $N(\gamma)$ are obtained. The ratio of these densities of states is a direct measure of the many-body renormalization, $G^0 = N(\gamma)/N(\chi) - 1$.³ Unfortunately, orbital contributions to the susceptibility make it very difficult to determine its spin component precisely in high-conductivity systems and phonon contributions to the specific heat can introduce significant systematic errors in the measurement of $N(\gamma)$. In this report we address the determination of G^0 and the spin-orbit scattering rate via the Pauli-limited, normal-state pairing resonance.¹⁰⁻¹³

If a paramagnetic system has a superconducting phase and can be made into a thin-film form, then it is possible to access the spin parameters through tunneling density-of-states (DOS) measurements. A Zeeman splitting of the BCS coherence peaks can be induced by applying a parallel mag-

netic field to a film of thickness $t \ll \xi$, where ξ is the superconducting coherence length. Tedrow and Meservey pioneered the use of superconducting spin-resolved tunneling to directly measure both spin-orbit scattering rate and the Landau parameter G^0 in thin Al and Ga films near the parallel critical-field transition.^{1,14,15} This technique, however, cannot access G^0 well into the superconducting phase since those electrons responsible for the exchange effects are consumed by the formation of the condensate.¹⁶ To circumvent this limitation, one needs to measure the Zeeman splittings in magnetic fields just below parallel critical field. However, one cannot completely reach the normal-state quasiparticle density in a thin film while remaining in the superconducting phase since the spin-paramagnetically limited parallel critical-field transition is first order. Because of this, one must extrapolate the normal-state value of G^0 from data taken in the superconducting phase. Alternatively, the films can be made marginally thicker, which will suppress the first-order transition,¹⁶ or the measurements can be made at higher temperatures. But these strategies limit one to a very narrow range of film thicknesses. Furthermore, in both cases one is constrained to a very narrow range of applied fields.

Here we present a detailed analysis of the normal-state pairing resonance (PR) from which the spin-orbit scattering rate, orbital depairing parameter, and the Landau parameter G^0 can be accurately obtained. We show that the technique can be used over a wide range of film thicknesses and resistances. Moreover, the measurements can be made in fields well above the parallel critical field and in fields substantially tilted away from parallel orientation.^{17,18}

II. PAIRING RESONANCE IN PARALLEL FIELD

The PR is characterized, as any other resonance, by two quantities: its position and its width. The former is given by¹¹

$$E_+ = \frac{1}{2}(E_Z + \Omega), \quad (1)$$

where

$$E_Z = \frac{2\mu_B H}{1 + G^0} \quad (2)$$

92
93 is the Zeeman energy renormalized by the Fermi-liquid pa-
94 rameter G^0 , μ_B is the Bohr magneton, and

$$\Omega = \sqrt{E_Z^2 - \Delta_0^2} \quad (3)$$

96 is the Cooper-pair energy with Δ_0 the zero-field, zero-
97 temperature gap of the corresponding superconducting
98 phase.

99 The width of the PR depends on the effective dimension-
100 ality of the sample and on the strength Γ of pair-breaking
101 mechanisms other than the Zeeman splitting. If these are
102 absent, a nonperturbative approach is necessary (see Ref.
103 11), and for quasi-two-dimensional systems the width is

$$W_2 = \frac{\Delta_0^2}{4g\Omega}, \quad (4)$$

105 where $g = 4\pi\hbar\nu_0 D$ is the dimensionless conductance with D
106 the diffusion constant and ν_0 the bare DOS. If $W_2 \ll \Gamma$ then a
107 perturbative calculation is sufficient to accurately estimate
108 the width, provided one properly takes into account the role
109 of the exclusion principle.¹⁸ For instance, in the case of a
110 tilted magnetic field, Γ is proportional to the perpendicular
111 component of the field and the exclusion principle both shifts
112 and reshapes the PR. If we consider the effects of spin-orbit
113 scattering and the finite-thickness orbital contributions of the
114 parallel field,¹⁹ then

$$\frac{\Gamma}{2\Delta_0} = b + c \left(\frac{\mu_B H}{\Delta_0} \right)^2, \quad (5)$$

116 where according to the notation commonly used to charac-
117 terize the DOS in the superconducting state,²⁰

$$b = \frac{\hbar}{3\tau_{so}\Delta_0} \quad (6)$$

119 is proportional to the spin-orbit scattering rate $1/\tau_{so}$ and

$$c = \frac{De^2 t^3 \Delta_0}{8\ell \mu_B^2 \hbar} \quad (7)$$

121 is the orbital depairing parameter, where t is the film's thick-
122 ness, e is the electron charge, and ℓ is the mean-free path.
123 This latter parameter quantifies the strength of the orbital
124 effect of the field²¹ in relation to the Zeeman effect. The
125 Zeeman splitting is the dominant pair-breaking mechanism
126 for $c \leq 1$.

127 Following the procedure outlined in Ref. 18, we obtain
128 the zero-temperature correction to the (spin-down) DOS due
129 to the PR

$$\frac{\delta\nu(\epsilon)}{\nu_0} = -A(\epsilon; E_Z, \Gamma) \frac{W_2 \Gamma}{(\epsilon - E_+)^2 + \Gamma^2}, \quad (8)$$

131 where ϵ is the energy measured from the Fermi level; the
132 other quantities entering this formula have been defined
133 above, see Eqs. (1)–(5). The correction for the other spin
134 component is found by replacing $\epsilon \rightarrow -\epsilon$ in the right-hand
135 side of Eq. (8). The function

$$A(\epsilon; E_Z, \Gamma) = \frac{1}{\pi} \{ \arctan[(E_Z - \epsilon)/\Gamma] + \arctan[\Omega/\Gamma] \\ + \arctan[(\epsilon - \Omega)/\Gamma] + \arctan[(2\epsilon - E_Z)/\Gamma] \} \quad (9) \quad 137$$

accounts for the exclusion principle and takes on values be-
138 tween 0 and 2. It alters the Lorentzian shape of the PR,
139 especially at energies close to the Fermi energy (i.e., $\epsilon \ll E_+$)
140 and, in fact, $A(\epsilon=0)=0$. We note that Eqs. (8) and (9) imply
141 that $\delta\nu/\nu_0 \leq 2W_2/\Gamma$, which is consistent with the assumed
142 perturbative criterion $\Gamma \gg W_2$.
143

In this work we show that Eq. (8) gives a quantitative
144 description of the PR and that it enables us to extract from
145 normal-state measurements the physical quantities G^0 , b , and
146 c . While they can be obtained from DOS measurements in
147 the superconducting state,^{15,16} this requires to solve a set of
148 self-consistent equations for the order parameter and “mo-
149 lecular” magnetic field together with the Usadel equations
150 for the normal and anomalous Green’s functions—a much
151 more complicated task in comparison to the simple fitting of
152 the data that we describe in Sec. IV.
153

III. EXPERIMENTAL PROCEDURE 154

Aluminum films were grown by e-beam deposition of
155 99.999% Al stock onto fire-polished glass-microscope slides
156 held at 84 K. The depositions were made at a rate of
157 ~ 0.1 nm/s in a typical vacuum $P < 3 \times 10^{-7}$ Torr. A series
158 of films with thicknesses ranging from 2 to 2.9 nm had a
159 dimensionless normal-state conductance that ranged from g
160 $= 5.6$ to 230 at 100 mK. After deposition, the films were
161 exposed to the atmosphere for 10–30 min in order to allow a
162 thin native oxide layer to form. Then a 9-nm-thick Al coun-
163 terelectrode was deposited onto the film with the oxide serv-
164 ing as the tunneling barrier. The counterelectrode had a par-
165 allel critical field of ~ 2.7 T due to its relatively large
166 thickness, which is to be compared with $H_{c||} \sim 6$ T for the
167 films. The junction area was about 1 mm \times 1 mm, while the
168 junction resistance ranged from 10–100 k Ω , depending on
169 exposure time and other factors. Only junctions with resis-
170 tances much greater than that of the films were used. Mea-
171 surements of resistance and tunneling were carried out on an
172 Oxford dilution refrigerator using a standard ac four-probe
173 technique. Magnetic fields of up to 9 T were applied using a
174 superconducting solenoid. A mechanical rotator was em-
175 ployed to orient the sample *in situ* with a precision of $\sim 0.1^\circ$.
176

IV. RESULTS AND DISCUSSION 177

We show in Fig. 1 the tunneling conductance measured at
178 70 mK and three supercritical parallel magnetic fields. This
179 particular film of dimensionless conductance $g \approx 57$ was 2.6
180 nm thick and had a zero-field superconducting transition
181 temperature $T_c = 2.74$ K. Common to the three data sets is
182 the Coulomb zero-bias anomaly (ZBA),²² which produces a
183 logarithmic depletion in the DOS at high biases; the loga-
184 rithm is cutoff at low bias by temperature. In order to isolate
185 the paramagnetic resonance, we need to remove the contri-
186

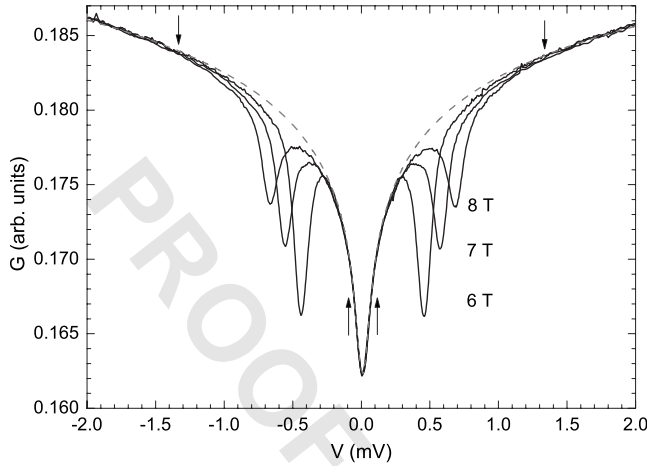


FIG. 1. Tunneling conductance at 70 mK for three supercritical parallel magnetic fields (solid lines). The dashed line is the fit to the zero-bias anomaly due to Coulomb interaction. The arrows point to the boundaries of the low- ($|V| \leq 0.2$ mV) and high-bias ($|V| \geq 1.4$ mV) regions used for the fitting.

187 bution of the ZBA. To interpolate between the low- and high-
 188 bias parts of the curves (as delimited by the arrows in Fig. 1),
 189 we find the best-fit curve, restricted to these regions, given
 190 by the sum of a background constant tunneling conductance
 191 and $\text{Re} \Psi(1/2 + i\alpha V)$, where Ψ is the digamma function and
 192 α a fitting parameter. The result is the dashed curve in Fig. 1,
 193 which is then subtracted from the measured tunneling con-
 194 ductances.

195 In Fig. 2 we plot with a solid line the PR at 7 T obtained
 196 as described above. As discussed in Sec. II, its position and
 197 width are, respectively, determined by the Zeeman energy E_Z
 198 and the pair-braking rate Γ while the conductance g only
 199 affects the overall magnitude. Using Eq. (8), the best fit to
 200 the data is given by the dot-dashed curve; while the main
 201 peak is well reproduced, a shoulder feature at higher bias is
 202 underestimated. To our knowledge, there are two possible

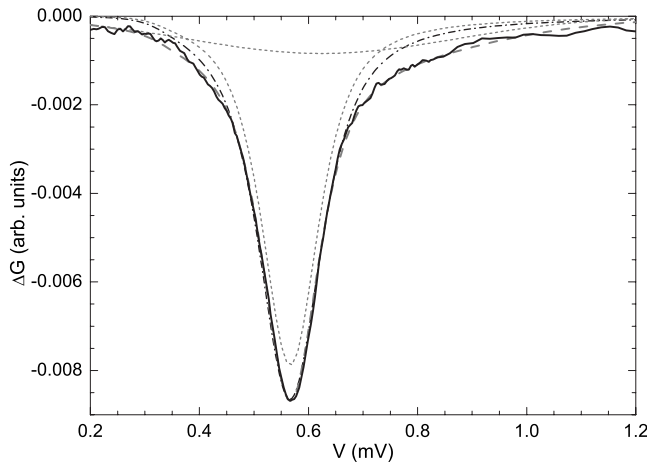


FIG. 2. Pairing resonance at 7 T (solid line) with the ZBA subtracted off. The dot-dashed curve is the best fit to the data using Eq. (8). The dashed curve is the best fit with a sum of Eq. (8) and a Gaussian—see the text for more details on the fitting procedure. The two terms of the sum are plotted separately as dotted curves.

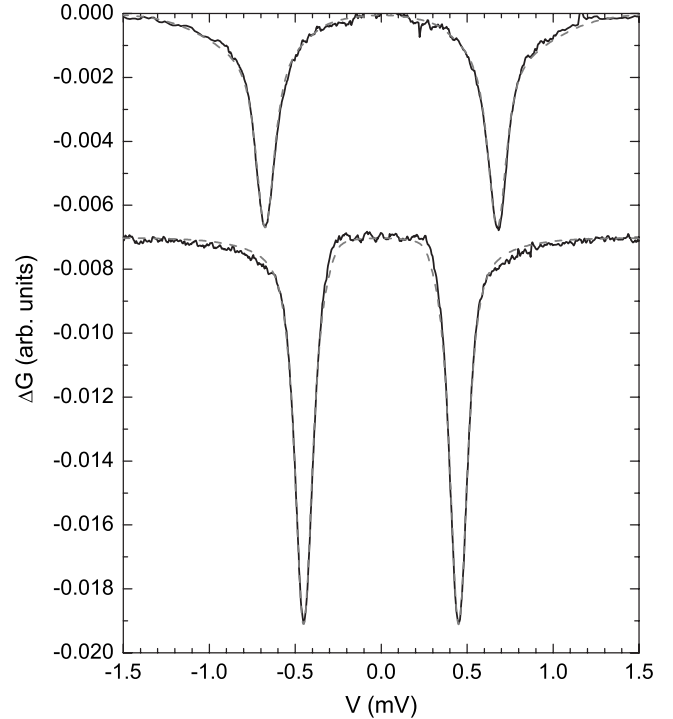


FIG. 3. Pairing resonances measured at 8 T (top) and 6 T (bottom solid curve). The bottom curve is shifted down by 0.007 for clarity. The dashed lines are best fits to the data obtained as described in the text. The asymmetry of the PR and its suppression near the Fermi energy are easily recognized in the data taken at 6 T.

causes for this discrepancy, namely, a finite bias, triplet chan- 203
 nel anomaly,²² similar to the Coulomb ZBA but much 204
 weaker, and finite-temperature effects.²³ To take into account 205
 these possible corrections, we add to Eq. (8) a Gaussian con- 206
 tribution; to reduce the number of free parameters, we re- 207
 quire it to be centered at the Zeeman energy, which is where 208
 a triplet channel correction would be located, while the am- 209
 plitude and width are used as fitting parameters. The best fit 210
 thus found is the dashed line in Fig. 2; the peaked PR and 211
 broad Gaussian contributions are plotted separately with dot- 212
 ted lines. 213

We present in Fig. 3 two more PRs with the best-fit 214
 curves. The asymmetric shape of the resonance and its sup- 215
 pression near the Fermi energy are evident in the lowest-field 216
 data. We note that fitting these data with Eq. (8) only would 217
 require us to decrease the conductance with increasing field, 218
 whereas we can use the same value of the conductance at all 219
 fields when the Gaussian correction is included. Moreover, 220
 the value of the Zeeman energy is only weakly affected by 221
 the inclusion of this correction, with the change in E_Z smaller 222
 than our estimated relative error of about 1%. While these 223
 two observations support the validity of our approach, the 224
 magnitude of the width parameter Γ turns out to be more 225
 sensitive to the Gaussian correction. However, its field depen- 226
 dence (see Fig. 5) is robust and the quantitative estimates 227
 discussed below are in line with expectations. 228

Having detailed our fitting procedure, we now consider 229
 the physical quantities that can be extracted from the data. In 230
 Fig. 4 we plot the normalized Zeeman energy as a function 231

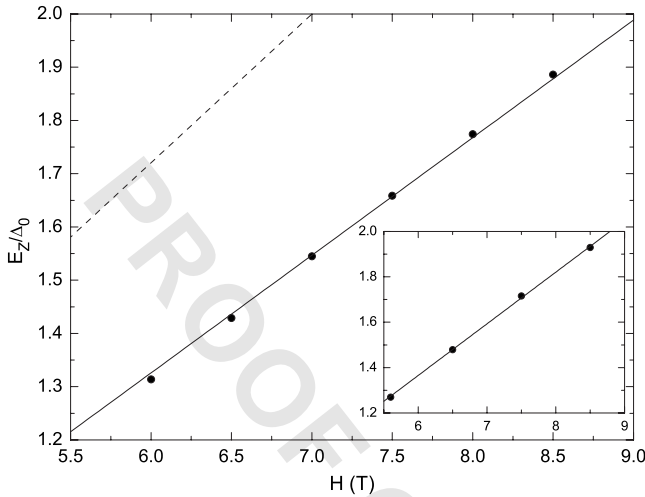


FIG. 4. Normalized Zeeman energy E_Z/Δ_0 vs magnetic field H . The solid line is the best fit to Eq. (2); the slope is proportional to $(1+G^0)^{-1}$ and we estimate the value of the Fermi-liquid parameter $G^0 \approx 0.26$. For comparison, the dashed line represents the expected linear relationship in the absence of Fermi-liquid renormalization. Inset: same plot as the main figure but for a thicker film with $G^0 \approx 0.24$ (see text for details).

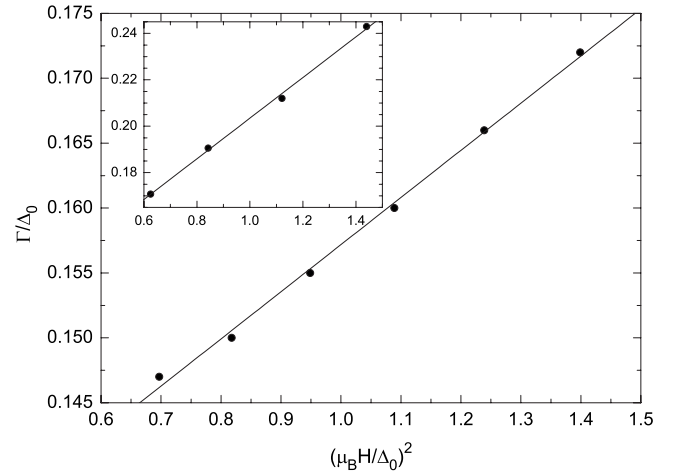


FIG. 5. Normalized pair-breaking parameter Γ/Δ_0 vs the square of the reduced field. Using the linear relationship in Eq. (5) we obtain from the best-fit line the spin-orbit scattering rate $b \approx 0.06$ and the orbital effect parameter $c \approx 0.02$. As in Fig. 4, we show in the inset the data pertaining to the 2.9-nm-thick film.

232 of the applied field. By fitting the data with Eq. (2) we find
 233 $G^0 \approx 0.26$; a similar estimate, $G^0 \approx 0.24$, is obtained for a
 234 thicker film with $t=2.9$ nm, $g=230$, and zero-field, zero-
 235 temperature gap $\Delta_0=0.41$ meV, see the inset of Fig. 4. We
 236 note that a better fit to the data in Fig. 4 could be obtained by
 237 allowing for a finite negative intercept; however, the large
 238 estimated error on the intercept makes the best-fit line com-
 239 patible with the expectation that it passes through the origin
 240 [see Eq. (2)]. This finite intercept could be due to small
 241 higher-order contributions since at the lowest field the pa-
 242 rameter $2W_2/\Gamma \approx 0.07$ is only marginally smaller than 1. In
 243 support to this interpretation, we find no evidence of finite
 244 intercept for the thicker film for which $2W_2/\Gamma \leq 0.016$. Al-
 245 ternatively, the intercept could be an additional indication,
 246 together with the shoulder feature mentioned above, of
 247 finite-temperature effects. We will further investigate this lat-
 248 ter issue in a separate work.

249 The width parameter Γ is plotted in Fig. 5 as a function of
 250 $(\mu_B H/\Delta_0)^2$ together with the best-fit line. According to Eq.
 251 (5), the intercept and the slope are determined by the spin-
 252 orbit parameter b and orbital parameter c , respectively. We
 253 estimate their values as $b \approx 0.06$, in agreement with the re-
 254 sults in the literature, and $c \approx 0.02$, which favorably
 255 compares²⁴ with the value $c \approx 0.04$ extrapolated from
 256 superconducting-state measurements in marginally thick
 257 (i.e., $c \approx 1$) films. Repeating the analysis for the thicker
 258 film—see the inset of Fig. 5—we find $b \approx 0.06$ and c
 259 ≈ 0.04 . As a further check on the validity of the present
 260 approach, for this film we show in Fig. 6 the measured and
 261 calculated DOS in the normal and superconducting states for
 262 fields of 5.6 and 4 T, respectively: all the main features of the
 263 superconducting DOS are captured by the theoretical curve²⁵
 264 obtained by solving the Usadel and self-consistent
 265 equations¹⁵ with the parameters found via the normal-state
 266 measurements.

In summary, we have presented a quantitative study of the
 paramagnetic pairing resonance in parallel field. We have
 derived an expression, Eq. (8), for the density of states which
 takes into account spin-orbit scattering, orbital effect of the
 magnetic field, and the Pauli exclusion principle. The latter is
 responsible for the suppression of the resonance near the
 Fermi energy, see Fig. 3 and the left panel of Fig. 6. By
 fitting the PRs measured at different fields we have obtained
 the values of the Fermi-liquid parameter G^0 , the spin-orbit
 scattering rate b , and the orbital parameter c , thus showing
 that normal-state experiments can provide the same informa-
 tion usually extracted from the DOS of the superconducting
 phase. Since the PR affects the spin-resolved DOS at oppo-
 site biases, it can, in fact, be used to probe the electron-spin
 polarization in magnetic films. The present work provides
 the foundation for the analysis of tunneling studies of itiner-
 ant magnetic systems via the PR.

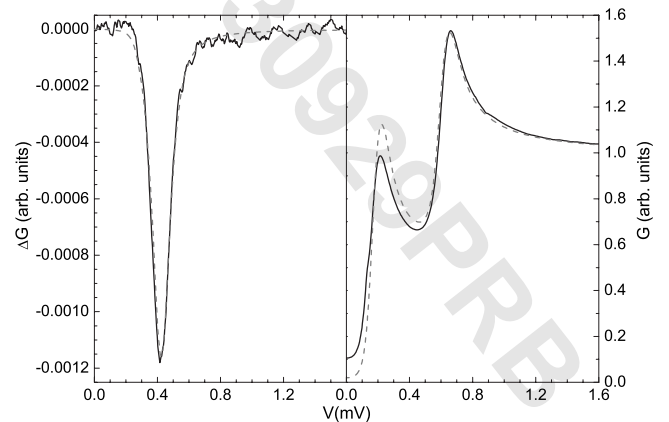


FIG. 6. Tunneling DOS in the normal (left, $H=5.6$ T) and superconducting (right, $H=4$ T) states at $T=70$ mK for a 2.9-nm-thick film. Solid lines are experimental data; dashed lines have been calculated with the parameters given in the text.

284 ACKNOWLEDGMENTS

285 We gratefully acknowledge enlightening discussions with
286 Ilya Vekhter and Dan Sheehy. This work was supported by

the DOE under Grant No. DE-FG02-07ER46420 for the ex- **287**
 perimental portion and by NSF under Grant No. NSF-DMR- **288**
 0547769 (GC). **289**

290
291
292

- 293** *Present address: School of Physics, Georgia Institute of Technol-
294 ogy, Atlanta, Georgia 30332, USA.
295 ¹G. A. Gibson, P. M. Tedrow, and R. Meservey, Phys. Rev. B **40**,
296 137 (1989).
297 ²D. C. Vier, D. W. Tolleth, and S. Schultz, Phys. Rev. B **29**, 88
298 (1984).
299 ³G. Baym and C. Pethick, *Landau Fermi-Liquid Theory: Con-*
300 *cepts and Applications* (John Wiley & Sons, New York, 1991).
301 ⁴A. J. Leggett, Phys. Rev. **140**, A1869 (1965).
302 ⁵B. L. Altshuler, A. G. Aronov, M. E. Gershenson, and Yu. V.
AQ: #03 Sharvin, Sov. Sci. Rev., Sect. A **9**, 223 (1987).
1 **304** ⁶G. Bergmann and C. Horriar-Esser, Phys. Rev. B **31**, 1161
305 (1985).
AQ: #06 ⁷A. P. Mackenzie and Y. Maeno, Rev. Mod. Phys. **75**, 657 (2003).
2 **307** ⁸I. L. Aleiner, D. E. Kharzeev, and A. M. Tsvelik, Phys. Rev. B
308 **76**, 195415 (2007).
309 ⁹L. P. Gor'kov and E. I. Rashba, Phys. Rev. Lett. **87**, 037004
310 (2001).
311 ¹⁰W. Wu, J. Williams, and P. W. Adams, Phys. Rev. Lett. **77**, 1139
312 (1996).
313 ¹¹I. L. Aleiner and B. L. Altshuler, Phys. Rev. Lett. **79**, 4242
314 (1997); H. Y. Kee, I. L. Aleiner, and B. L. Altshuler, Phys. Rev.
315 B **58**, 5757 (1998).
316 ¹²V. Y. Butko, P. W. Adams, and I. L. Aleiner, Phys. Rev. Lett. **82**,
317 4284 (1999).
318 ¹³P. W. Adams and V. Y. Butko, Physica B **284-288**, 673 (2000).
319 ¹⁴P. M. Tedrow, J. T. Kucera, D. Rainer, and T. P. Orlando, Phys.
 Rev. Lett. **52**, 1637 (1984). **320**
¹⁵J. A. X. Alexander, T. P. Orlando, D. Rainer, and P. M. Tedrow,
 Phys. Rev. B **31**, 5811 (1985). **321**
¹⁶G. Catelani, X. S. Wu, and P. W. Adams, Phys. Rev. B **78**, **323**
 104515 (2008). **324**
¹⁷X. S. Wu, P. W. Adams, and G. Catelani, Phys. Rev. Lett. **95**, **325**
 167001 (2005). **326**
¹⁸G. Catelani, Phys. Rev. B **73**, 020503(R) (2006). **327**
¹⁹In principle, inelastic-scattering effects should also be included.
 However, their contribution to the width Γ can be neglected; this **328**
 point is discussed in some detail in Ref. **11**. **329**
²⁰P. Fulde, Adv. Phys. **22**, 667 (1973). **330**
²¹This definition is applicable in the limit $t \ll \ell$ of interest here. **331**
²²B. L. Altshuler and A. G. Aronov, in *Electron-Electron Interac-*
tion in Disordered Systems, edited by A. L. Efros and M. Pollak
 (North-Holland, Amsterdam, 1985). **332**
²³We note that the small finite-temperature broadening due to the
 usual convolution with the derivative of the Fermi-Dirac distri-
 bution function has been taken into account. **333**
²⁴The actual film thickness is less than the nominal one due to the
 oxidation (see Sec. **III**) and extrapolation from thicker films
 overestimates c . **334**
²⁵In calculating the superconducting DOS we have introduced a
 small broadening of the same order of magnitude used in Ref.
16. **335**
²⁶Y. M. Xiong, P. W. Adams, and G. Catelani, Phys. Rev. Lett. (to
 be published). **336** **AQ**
#3

AUTHOR QUERIES —

- #1 Au: Please verify the changes made in journal title in Ref. 5.
- #2 Au: The first page should be '657' not '675' in the Ref. 7. Please verify.
- #3 Au: Please update Ref. 26 if possible.

PROOF COPY [BE11055] 030929PRB